European Journal of Agronomy 97 (2018) 28–37

Contents lists available at ScienceDirect

European Journal of Agronomy

journal homepage: www.elsevier.com/locate/eja

SuMoToRI model simulations for optimizing sulphur fertilization in oilseed rape in the context of increased spring temperatures

E. Poisson[a,*], A. Mollier[b], J. Trouverie[a], J.-C. Avice[a], S. Brunel-Muguet[a]

[a] EVA, Normandie Univ, UNICAEN, INRA, 14000, Caen, France
[b] ISPA, Bordeaux Sciences Agro, INRA, 33140, Villenave d'Ornon, France

ARTICLE INFO

Keywords:
Crop model
Sulphur
Oilseed rape
Temperature
Climate change
Simulation

ABSTRACT

For the last few decades, environmental policies have led to drastic reduction in sulphur (S)-containing industrial emissions leading to reduced S inputs into the soil. This is of concern for oilseed rape (*Brassica napus* L.), which like most Brassica species is a high S-demanding crop. In this context, monitoring S fertilization has become a central issue. Moreover, ongoing and projected climate change will affect crop yield and quality worldwide, thus justifying the prediction of climate effects via modelling approaches so that crop management and practices can be adjusted. In this modelling study, the growth and S status of winter oilseed rape (WOSR) were investigated from the end of winter until the onset of pod formation under contrasting S supplies in a range of climatic conditions acquired for seven major WOSR-producing northern countries and under the four Representative Concentration Pathway (RCP) scenarios (i.e. RCP2.6, RCP4.5, RCP6.0, and RCP8.5). Simulations were performed with the process-based model SuMoToRI (*Sulphur Model Towards Rapeseed Improvement*) for past datasets (1948–2005) and projections (2015–2099). Simulation results indicated decreased plant biomass (mainly leaves) as temperatures increased (as expected under the increasingly negative scenarios as the century progresses) and as daily incident radiation decreased in contrast to the mobile S of leaves (mainly sulphate), which tended to accumulate as a consequence of reduced S sink (i.e. leaves) size. These simulations highlighted the increased risks of S over-fertilization, which can lead to environmental issues that mainly comprise S leaching due to high mobile-S in leaves that senesce. Overall, this *in silico* study raises questions about the most suitable S fertilization strategies and associated farming practices for dealing with the expected adverse climatic conditions.

1. Introduction

Sulphur (S) oligotrophy has become a matter of concern during the last four decades, not only as a consequence of drastic environmental policies aiming to reduce sulphur dioxide in industrial emissions (Schnug and Evans, 1992), but also because of the substitution of S-containing nitrogen (N) and phosphorus (P) fertilizers (Scherer, 2001) and of the reduction in S-containing fungicides with alternative compounds that contain no or only small amounts of S (Zhao et al., 1999). This has led to reductions in "free" S deposition into the soil, which has negatively impacted arable land (McGrath et al., 2002; Scherer, 2001; Schnug et al., 1993). This issue has been of concern especially in oilseed rape, the third most important oilseed crop on an oil production basis (FAO, 2014). Like most of the *Brassicaceae*, oilseed rape is a high S-demanding crop whose requirements are up to four times those of wheat (Oenema and Postma, 2003). Oilseed rape is mainly grown for oil (ca. 40% of fatty acids (FAs) on a seed dry matter (DM) basis) used for human consumption and biodiesel® production and for protein-rich meals (ca. 35% of proteins on a seed DM basis) that are the by-products of oil extraction and mainly used for cattle feeding and other industrial derivatives (Von Der Haar et al., 2014). Extended S-limiting periods that occur during early stages were shown to negatively impact yield components (e.g. seed yield, thousand seed weight, pod number), and oil and meal quality characteristics (e.g. fatty acid (FA) content and distribution, protein content and seed storage protein (SSP) composition) (D'Hooghe et al., 2014; Dubousset et al., 2010). Consequently, S fertilization management has recently gained attention to prevent yield penalties and decreased oil and meal quality. In addition, ongoing and projected climate change will affect crop yield and quality worldwide, thus threatening global food security (Godfray et al., 2010; Sundström et al., 2014; Tubiello et al., 2007). Interactions between climatic variables such as temperature, radiation, rainfall, elevated CO_2 and fertilization are widely documented, thereby justifying a tight monitoring of fertilization in the context of climate variability (Ross et al., 2004; Schneider et al., 2004). In oilseed rape, recent work has indicated additional, opposite and interactions effects between increased

* Corresponding author.
E-mail addresses: emilie.poisson@unicaen.fr (E. Poisson), sophie.brunel-muguet@unicaen.fr (S. Brunel-Muguet).

https://doi.org/10.1016/j.eja.2018.05.001
Received 22 November 2017; Received in revised form 30 March 2018; Accepted 2 May 2018
Available online 12 May 2018

temperature during the grain filling period and S availability (Brunel-Muguet et al., 2015a). This then raises questions about the timing and the amount of S supply that is adequate for optimizing yield and seed quality when the plants are challenged with warmer spring temperatures. For instance, S limitation and heat stress during seed filling have opposite impacts on the total seed FA content (i.e. increase under heat stress vs. decrease under S limitation, respectively) and the S-rich/S-poor protein ratio in seeds (i.e. increase in the ratio under heat stress vs. a decrease in the ratio under S limitation) (Brunel-Muguet et al., 2015a). Temperature and S supply interactions were observed for seed yield (total seed biomass), which is reduced under heat stress and non-limiting S conditions and increased under both stresses. These results underline the importance of considering the effects of S nutrition and increased spring temperatures together.

In the context of increasing climate variability, the impacts of environmental factors and plant nutrition need to be predicted in order to deliver crop fertilization strategies that have a better fit with future climate patterns. Process-based crop models have emerged as relevant tools to simulate plant performance in a wide range of environmental conditions. Most process-based crop models allow quantitative estimation of plant responses to climate related variables (e.g. temperature, radiation, atmospheric CO_2, rainfall) and nutrient availability. The roles of these models have been discussed recently with questions about their efficiency and the need to upgrade their function to better account for climatic variability such as increases in the frequency of extreme events (Challinor et al., 2017; Chenu et al., 2017; Maiorano et al., 2017; Ruane et al., 2016; Tubiello et al., 2007; Wang et al., 2017).

In this study we used the process-based model SuMoToRI (Sulphur Model Towards Rapeseed Improvement) (Brunel-Muguet et al., 2015b), which simulates the dynamics of growth, S allocation among plant compartments (i.e. leaves *in planta*, detached leaves, and the rest of the plant) and S partitioning (i.e. the fraction of mineral vs. organic S) within each plant compartment from the end of the vegetative rest period until the onset of pod formation. Predictions of the mineral S pool (mobile) in the leaves at this stage were used as an indicator of the potential for S remobilization towards pods and seeds. Our objectives were twofold. The first aim was to predict plant performance under two contrasting S supplies i.e. High Sulphur availability (HS) and Low Sulphur availability (LS) under a wide range of environmental conditions across seven locations distributed across the northern hemisphere and under four climatic scenarios that followed assessments by the Intergovernmental Panel on Climate Change (IPCC) (IPCC, 2014). Secondly, we aimed to unravel the impact on plant performance at the onset of the reproductive phase of the three environmental factors captured in the model i.e. temperature, incident radiation (associated with climate change, and thus variable according to location and climatic scenario) and plant S availability. Ultimately, these simulations aimed to give insights into S fertilization strategies and varieties that will be better adapted to climatic change during the course of this century.

2. Material and methods

2.1. Description of the SuMoToRI crop model

Briefly, the process-based model SuMoToRI (Brunel-Muguet et al., 2015b) predicts the dynamics of the Leaf Area Index (LAI), biomass, and the amounts of organic and mineral S in three plant compartments i.e. leaves *in planta* (described as a single big leaf (BL)), detached leaves and the rest of the plant (i.e. stems, flowers, young pods, the roots and taproot), from the end of the vegetative rest period until the onset of pod formation (GS70, Lancashire et al., 1991). Outputs are driven by the three environmental factors considered within the model on a daily time step i.e. temperature, incident radiation and the amount of S taken up. The original features of the model rely on (i) the determination of the S requirements used for growth (structural and metabolic functions) through critical S dilution curves determined for the leaves *in planta* and the rest of the plant and (ii) the estimation of a mobile pool of S (i.e. the mineral S compounds, mainly sulphates) that is regenerated by daily S uptake and remobilization from senescing leaves before they detach. Because leaves are the main storage organs and sulphate is the main S-storage form during the vegetative phase, the prediction of S mineral content in leaves allows determination of the potential for S remobilization towards growing sinks (i.e. pods and seeds) as a proxy of the plant's ability to satisfy S requirements throughout the reproductive phase. The model is run on a daily time step with a limited number of plant parameters, most with generic values irrespective of the plant S availability. These parameters refer to the potential leaf growth, carbon (C) plant offer and C demand by the leaves, as well as S allocation (among compartments) and partitioning (organic vs. mineral) (Brunel-Muguet et al., 2015b). The two contrasting S supplies refer to values that were used to calibrate the model (Brunel-Muguet et al., 2015b). The high and low S supplies account for 120 and 20 units of S, respectively, which were provided at the bolting stage at the end of winter (Terres Inovia, http://www.terresinovia.fr/colza/cultiver-du-colza/fertilization/soufre/).

2.2. Data sources and simulation analysis design

2.2.1. Selection of locations

Seven locations in oilseed rape-producing countries were selected in the northern hemisphere in order to have a wide range of climatic datasets (mainly temperature and radiation, which are both considered in the model) and the same cultivated oilseed rape type i.e. winter varieties (winter oilseed rape, WOSR, Table 1). These localities are the following: Chillicothe and Lincoln (34°15′N, 99°21′W and 40°49′N, 96°41′W respectively, USA), Crawley (51°6′N, 0°11′W, United Kingdom), Dijon (48°51′N, 2°17′E, France), Hurva (55°79′, 5°04′E, Sweden), Ternopil (49°33′N, 25°35′E, Ukraine) and Xianning (29°50′N, 114°19′E, China). These locations are characterized by contrasting annual daily mean temperature (Tmean_year), annual mean daily minimum and daily maximum temperatures (Tmin_year and Tmax_year), and annual mean daily incident photosynthetically active radiation (PARi_year) as reported during the past and predicted under projected climatic scenarios (Table 1 and Supplemental data Fig. A and B).

2.2.2. Description of the climatic scenarios and simulation periods

In this study, we aimed to estimate the impacts of the evolution of temperature and radiation on WOSR growth in each selected location and according to projected scenarios. Climatic scenarios for future emissions of major gases and aerosols have been generated for assessments by the Intergovernmental Panel on Climate Change (IPCC, 2014). The climatic scenarios represent various development pathways based on well-defined assumptions (van Vuuren et al., 2011). The scenarios are used to calculate future changes in climate, and are then archived in the Coupled Model Intercomparison Project (CMIP). In the fifth version of CMIP (CMIP5), four new scenarios, referred to as Representative Concentration Pathways (RCPs) have been developed. The four RCPs (RCP2.6, RCP4.5, RCP6.0, and RCP8.5) (Inman, 2011) are named after an expected range of radiative forcing values in the year 2100 relative to pre-industrial values ($+2.6$, $+4.5$, $+6.0$, and $+8.5\,W/m^2$, respectively). RCPs are a set of standards mainly used by climate modellers and provide a common, agreed reference for modelling climate change around the world. These four RCPs were used under one of the general circulation models (GCMs): IPSL-CM5a_mr from CMIP5 (Belda et al., 2015; Dufresne et al., 2013). Raw climate model outputs were calibrated by the Bias-Correction (with variability) method (BC) (Hawkins et al., 2013) using the Princeton observational dataset (Sheffield et al., 2006). The BC approach corrects the projected raw daily GCM output using the differences in the mean and variability between the GCM and observations in a reference period. The daily data is shifted by the mean

Table 1
Climatic characteristics of the seven locations distributed across the northern hemisphere. Minimal (Tmin_year), maximal (Tmax_year) and mean temperature (Tmean_year) correspond to the annual mean daily minimal, maximal and mean temperatures respectively (in °C). Incident PAR (PARi_year) corresponds to the mean daily incident PAR (in MJ/m^2). Historical values are given for 1948–2005 and values for the 4 RCPs are given for 2015–2099.

Location		Chillicothe	Lincoln	Crawley	Dijon	Hurva	Ternopil	Xianning
Country/State		USA/Texas	USA/ Nebraska	United Kingdom	France	Sweden	Ukraine	China
GPS coordinates		34°15′ N 99°31′ W	40°49′ N 96°41′W	51°6′ N 0°11′ W	48°51′N 2°17′E	55°47′N 13°26′W	49°33′N 25°35′E	29°50′N 114°19′W
Tmin_year	Historical	10	4.4	5.7	6.2	4.2	2.8	13.3
	RCP2.6	11.6	6.1	6.2	7.2	5.7	4.4	14.6
	RCP4.5	12.2	6.8	6.6	7.8	6.3	5.8	15.2
	RCP6.0	12.3	6.9	6.5	7.8	6.2	6.2	15.1
	RCP8.5	13.4	8.2	7.0	8.6	6.8	7.6	16.3
Tmax_year	Historical	24.6	17.4	13.5	14.9	11.1	11.9	21.3
	RCP2.6	26.2	18.9	14.2	16.4	12.8	13.6	23.3
	RCP4.5	26.9	19.5	14.6	17.1	13.4	15.3	23.9
	RCP6.0	27.1	19.8	14.5	17.1	13.3	15.7	23.6
	RCP8.5	28.3	21	15.1	18.2	14	17.3	24.8
Tmean_year	Historical	17.3	10.9	9.6	10.5	7.6	7.35	17.6
	RCP2.6	18.9	12.5	10.2	11.8	9.2	9	18.9
	RCP4.5	19.5	13.1	10.6	12.4	9.8	10.5	19.5
	RCP6.0	19.7	13.3	10.5	12.4	9.7	10.9	19.4
	RCP8.5	20.8	14.6	11	13.4	10.4	12.4	20.6
PARi_year	Historical	18.3	15.5	10.7	12.3	9.9	10.8	13.1
	RCP2.6	18.5	15.5	10.5	12.2	9.3	10.3	9.9
	RCP4.5	18.4	15.4	10.6	12.3	9.3	10.5	9.9
	RCP6.0	18.4	15.5	10.5	12.2	9.3	10.5	10
	RCP8.5	18.4	15.4	10.5	12.3	9.2	10.4	10.2

bias in the reference period, taking into account the temporal variability of the model output in accordance with the observations. Princeton is a meteorological forcing dataset constructed by combining a suite of global observation-based datasets with the NCEP/NCAR reanalysis. The dataset is available at 0.25 ° of resolution for 1948–2008. For the purpose of the simulations, we extracted daily average temperature and solar radiation from the CCAFS-Climate portal (http://ccafs-climate.org/data_bias_correction/) for the four scenarios from 2015 to 2099 and for a past period from 1948 to 2005, for each location. Increased annual mean temperatures over the coming decades are generally observed, whatever the location, and are even more pronounced under the most pessimistic scenarios (i.e. in gradual ranking: RCP2.6 < RCP4.5 < RCP6.0 < RCP8.5; Supplemental data Fig. A). For each location and each S supply condition, we performed simulations with climatic datasets for the past period (named “historical”) and with projected climatic datasets under the four RCPs (i.e. 5502 simulations in total).

2.2.3. Initialization of the model

In the model, the predictive period encompasses the stem elongation stage (GS30), which occurs at the end of winter until the onset of pod formation (GS70) (Lancashire et al., 1991). In order to initialize the model, prior determination of the date of the end of winter (EndW i.e. date of initialization of the model) was defined based on two criteria that deal with (i) the photoperiod (i.e. minimum daytime of 10.5 h) and (ii) temperature rules (i.e. at least 7 consecutive days above 8 °C). These criteria were determined based on observations of the dates of the EndW in two locations i.e. Saint-Martin-de-Hinx (43°34′N, 1°16′W, France) and Mont-en-Chaussée (49°52′N, 3°00′E, France), from 1950 to 2005 (data collected in the DRIAS portal, http://www.drias-climat.fr/). The criteria were adapted to match the usual period of regrowth, which is the time that S fertilizer is applied to the crop (Terres Inovia, http://www.terresinovia.fr/colza/cultiver-du-colza/fertilization/soufre/).
These EndW dates, expressed as calendar dates, differ for both southern and northern locations in the northern hemisphere, and this supports the importance of generalized criteria for determining the EndW date, regardless of the location. Therefore for each year (1948–2005 for the past period and 2015–2099 for the projected datasets) and each location, the EndW date was determined according to these criteria. With regard to the other initial state values, namely the leaf area (LA_{ini}), total and leaf dry weight (TDW_{ini}, LDW_{ini}), absorbed PAR ($PARabs_{ini}$), whole plant S taken up ($QStot_{ini}$) and the S amount in the leaves ($QSleaves_{ini}$), we used the respective values of the model parameterization under the HS and LS conditions (Brunel-Muguet et al., 2015b, Supplemental data Table A). The simulations were performed with a single set of parameter values for HS and LS conditions obtained after model calibration, except for the Radiation Use Efficiency (RUE) values, which differ according to S availability (Brunel-Muguet et al., 2015b, Supplemental data Table A).

2.2.4. Model outputs and statistical analyses

The Simulated End Date (SED) refers to the day of the year number when the plant reaches a cumulative thermal time (TT) of 950 °Cd after the end of winter, which is the TT requirement for the onset of pod formation (GS70) (calibrated according to Brunel-Muguet et al., 2015b). The SED indicates to what extent the onset of pod formation (GS70) is early according to the temperature, radiation and the S-related processes within the model. A single factor ANOVA was performed to test the effects of location or scenario on the SED for each scenario or for each location, respectively (STATGRAPHICS Centurion XVI.II Software). The difference in slope values of the linear regressions among localities and scenarios was tested with multiple regression analysis with a 95% confidence level (STATGRAPHICS Centurion XVI.II Software). The other main model outputs presented are the total and leaf dry weight (TDW, LDW), the leaf area index (LAI) and the amount of mobile S in the green leaves (QSmobile.GL) at the end of the simulation period (950 °Cd after the end of winter). A single factor ANOVA was performed to test the location or the scenario effect on the SED, TDW, LDW, LAI and QS.mobile.GL for each scenario or for each location respectively. Multiple comparison tests (LSD, 95% confidence level) were also performed to rank the locations based on the mean variables value for all scenarios gathered. Heat maps were generated

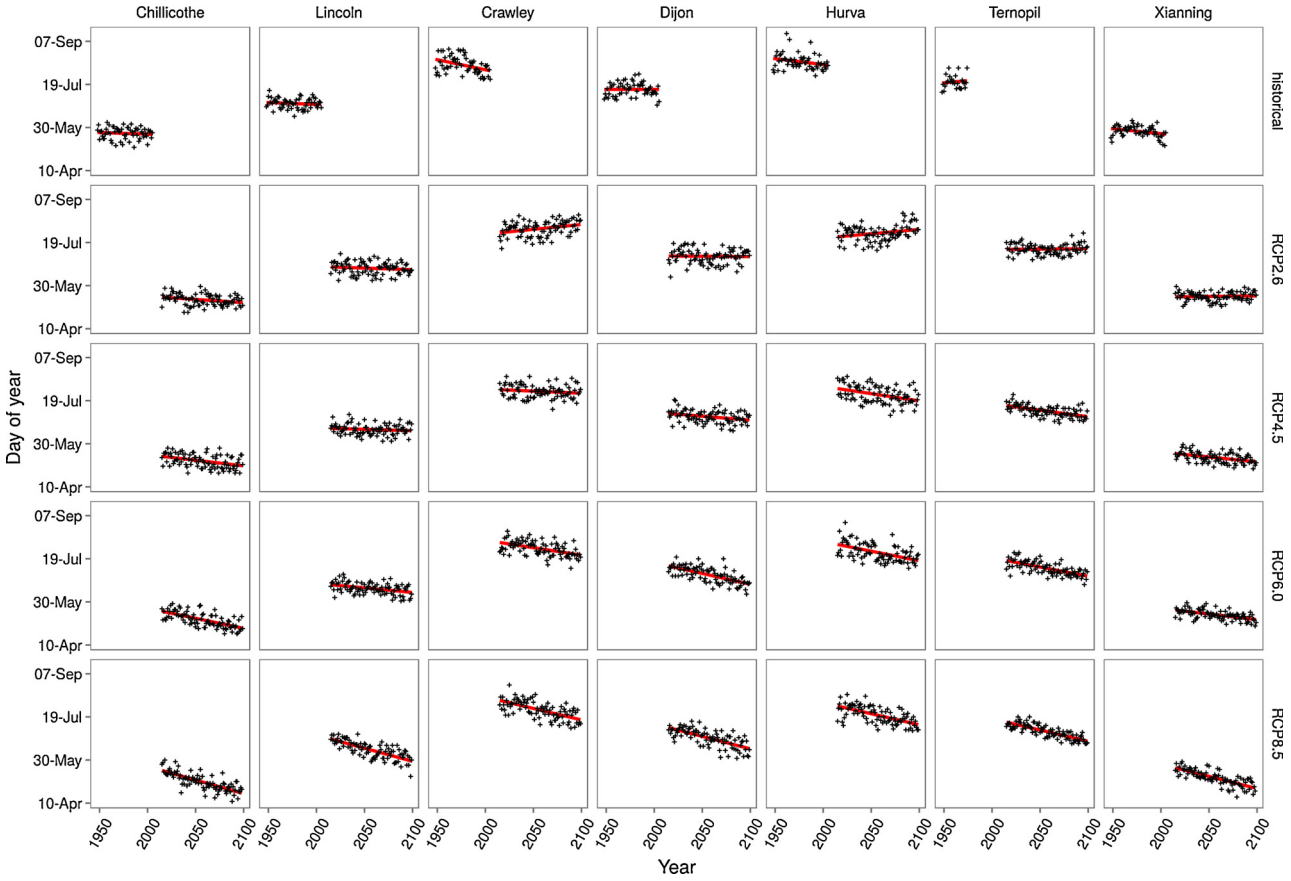

Fig. 1. Representation of the simulated end dates (SEDs) as a function of year under the historical dataset (1948–2005) and each scenario (RCP2.6, RCP4.5, RCP6.0, and RCP8.5) from 2015 to 2099 for each location (Chillicothe, Lincoln, Crawley, Dijon, Hurva, Ternopil and Xianning). The SEDs are expressed as the day number of the year. Lines represent the linear regressions.

with the R package ggplot from the R language environment for statistical computing, version 3.3.2 (R Development Core Team, 2014).

3. Results

3.1. Simulated end dates

Fig. 1 displays the SED as a function of the year for each location (Chillicothe, Lincoln, Crawley, Dijon, Hurva, Ternopil and Xianning) and under each scenario (RCP2.6, RCP4.5, RCP6.0, and RCP8.5, from 2015 to 2099) and the historical dataset (from 1948 to 2005). Table 2 gives the SED (expressed as the day number of the year), and the slopes and coefficients of determination (R^2) of the linear regressions (day number as a function of year), which indicate the earliness trends and the inter-annual variability, respectively. Regarding the SED, a significant location effect was observed with similar rankings under each scenario (Table 2). Three location groups can be distinguished (data not shown): Chillicothe and Xianning with early SEDs (mid-spring with day of year ranging between 125 and 146), Lincoln, Dijon and Ternopil with intermediate SEDs (late spring-early summer with day of year ranging between 161 and 203) and Hurva and Crawley with late SEDs (mid-summer with day of year ranging between 202 and 226) according to the scenarios. A significant scenario effect was also observed for each location with a decrease in SED along with a significant increase in the scenario intensity (in a gradual ranking RCP2.6 < RCP4.5 < RCP6.0 < RCP8.5). The slope values were most often negative (except for Crawley, Hurva, Ternopil and Xianning under RCP2.6), which meant that the day number of the year reached 950 °Cd earlier with the increases in daily mean temperature projected under each scenario and for each location (Supplemental data Fig. A). A location effect was observed as expected under RCP8.5, which is the most pessimistic scenario, while a highly significant scenario effect was observed for each location (Table 2). Whatever the location, the slope value increased when the scenario became more pessimistic. This trend points out the reduction in the number of days required to reach the onset of pod formation according to the scenario's intensity. Complementary to the earliness trends given by the SEDs and slope values, the coefficient of determination indicated the extent of the inter-annual variability in SED i.e. the lower the value, the higher the variability across years. The inter-annual variability tended to decrease (i.e. a higher value in R^2) under the most pessimistic scenarios with the highest R^2 value being under RCP8.5 followed by RCP6.0, RCP4.5 and RCP2.6, for a given location (Table 2). When comparing locations, the highest R^2 values were observed for Ternopil, Xianning, and Chillicothe, especially under RCP8.5, RCP6.0 and RCP4.5, meaning that the inter-annual variability in SED in these locations was lower than in the others, which is even more pronounced with pessimistic scenarios.

3.2. Plant performances at the onset of pod formation

The main plant performance outputs are related to growth (i.e. TDW, LDW in g/plant) and the potential for S remobilization using mobile S in the green leaves (QS.mobile.GL in mg/plant) as a proxy at the onset of pod formation. In the model we made the assumption that the accumulation of mobile S in the leaves before and throughout the reproductive phase drives the capacity of the plant to further provide S to newly grown sinks i.e. pods. Here, we only report TDW (and not LDW because the results are very close to LAI), LAI and QS.mobile.GL simulated at the SED (which is 950 °Cd after the end of winter) to illustrate the plant performance in terms of growth and S storage and

Table 2
Mean simulated end date (SED, expressed as the day number of the year), Slope, y-intercept and coefficient of determination of the linear regression between the year and the day number to reach the SED, for each location and scenario (average calculated over years). The mean day number was calculated over 1948–2005 for the historical dataset and over 2015–2099 for RCP2.6, RCP4.5, RCP6.0 and RCP8.5. The significance of the difference between the day number, the slopes and the y-intercepts were tested among locations for a given scenario and among scenarios (excluding the historical dataset) for a given location. Levels of significance: ns non-significant, * $p < 0.05$, ** $p < 0.01$, *** p 0.001.

Location	Chillicothe	Lincoln	Crawley	Dijon	Hurva	Ternopil	Xianning	
Scenario	SED (day number)							Location effect
Historical	143	178	222	194	226	203	146	***
RCP2.6	133	170	216	184	211	192	138	***
RCP4.5	130	166	211	181	207	188	134	***
RCP6.0	129	165	212	181	207	189	135	***
RCP8.5	125	161	208	175	202	183	129	***
Scenario effect	***	***	***	***	***	***	***	
Scenario	Slope *y-intercept*							Location effect
Historical	−0.04	−0.04	−0.23	0.00	−0.14	0.11	−0.11	ns
	213	*262*	*682*	*193*	*495*	*−5*	*373*	***
RCP2.6	−0.08	−0.04	0.11	−0.01	0.10	0.01	0.01	***
	288	*245*	*−16*	*200*	*3*	*176*	*111*	***
RCP4.5	−0.13	−0.03	−0.05	−0.09	−0.17	−0.15	−0.11	*
	397	*233*	*311*	*369*	*553*	*501*	*370*	***
RCP6.0	−0.23	−0.11	−0.17	−0.25	−0.22	−0.21	−0.13	**
	609	*382*	*566*	*702*	*606*	*630*	*407*	***
RCP8.5	−0.32	−0.30	−0.27	−0.29	−0.26	−0.26	−0.28	ns
	776	*788*	*757*	*772*	*729*	*718*	*711*	***
Scenario effect	***	***	***	***	***	***	***	
	***	***	***	***	***	***	***	
Scenario	R^2							
Historical	0.01	0.01	0.15	0.00	0.06	0.01	0.10	
RCP2.6	0.08	0.02	0.10	0.00	0.07	0.00	0.00	
RCP4.5	0.17	0.02	0.02	0.10	0.17	0.33	0.20	
RCP6.0	0.44	0.15	0.25	0.45	0.27	0.45	0.32	
RCP8.5	0.57	0.55	0.40	0.48	0.38	0.64	0.59	

remobilization capacity at the onset of pod formation.

3.2.1. Biomass simulations and leaf area expansion

Fig. 2a and Tables 3 and 4 present TDW values at the SED under the four scenarios and the past dataset for each location, under HS and LS. As expected higher values were observed in HS than in LS (*ca.* 50% higher), whichever scenario or location was considered. Under both S conditions, TDW tends to decline over the simulated years (Fig. 2a). Under HS, when comparing locations, three groups can be distinguished (data not shown): {Crawley and Dijon} with the highest values ranging from 163.9 to 188.5 mg/plant, Chillicothe, Lincoln, Hurva and Ternopil ranging from 132.3 to 157.2 mg/plant and Xianning ranging from 66.8 to 71.9 mg/plant for all the scenarios (Table 3). The same location ranking was observed under LS with Crawley and Dijon ranging from 81.8 to 85.7 mg/plant, Chillicothe, Lincoln, Hurva and Ternopil ranging from 65.7 to 78.8 mg/plant and Xianning ranging from 34.1 to 36.8 mg/plant for all scenarios (Table 4). For both S conditions, a scenario effect was observed with lower TDW because the scenario is more pessimistic, mainly in Chillicothe and Dijon under HS and Chillicothe and Ternopil under LS but not for Xianning, which displays higher TDW along with more pessimistic scenarios.

With regards to LAI, a location effect was also observed but with different location rankings compared to TDW (Fig. 2b and c, Tables 3 and 4). Under HS, LAI ranged from 7.192 to 7.196 m^2/m^2 for Lincoln, Xianning and Chillicothe, from 7.182 to 7.191 m^2/m^2 for Dijon and Ternopil and from 7.174 to 7.184 m^2/m^2 for Hurva and Crawley, for all the scenarios (Table 3). Under LS, values were *ca*. 30% lower than in HS with different location rankings: Chillicothe and Crawley ranging from 5.379 to 5427 m^2/m^2, Lincoln, Hurva, Ternopil and Dijon ranging from 5.366 to 5.415 m^2/m^2 and Xianning ranging from 5.351 to 5.425 m^2/m^2, for all the scenarios (Table 4). The same location trends were observed for LDW with lower values under HS and LS (*ca.* 30% lower) and similar location rankings to those for LDW under HS and LS, respectively (data not shown). LDW and LAI values also decreased over years. However, in contrast to TDW, no significant differences between scenarios were observed for a given location except for Dijon under HS and Chillicothe under LS (Tables 3 and 4).

3.2.2. S allocation and partitioning simulations

The amount of mobile S in the green leaves (QS.mobile.GL) is displayed in Fig. 2c and Tables 3 and 4. As expected, highly significant differences were observed between S conditions, with values *ca.* 90% lower in LS than in HS for all the locations and scenarios except for Xianning, which displayed values *ca.* 100% lower in LS than in HS (Tables 3 and 4). Similar to biomass performance, QS.mobile.GL values tended to decline over the simulated years (Fig. 2d).

When comparing locations, each location had significantly different values from the others under HS, with Xianning having the highest values (29.19–32.68 mg S-SO_4/plant) while they can be clustered into three groups under LS: Chillicothe, Lincoln and Ternopil ranging from 0.41 to 0.45 mg S-SO_4/plant, Dijon, Hurva and Crawley ranging from 0.37 to 0.40 mg S-SO_4/plant and Xianning ranging from 0.33 to 0.37 mg S-SO_4/plant, for all the scenarios. The scenario effect was only observed under HS, with a significant increase in QS.mobile.GL being observed for all the locations along with a significant increase in the scenario intensity, except for the case of Xianning, which displayed higher values (Tables 3 and 4).

4. Discussion

4.1. Respective effects of location and scenario on SED, total and leaf biomass

This *in silico* study sampled a broad range of environmental conditions in seven locations distributed across the north hemisphere and four climatic scenario datasets with the aim of simulating biomass and

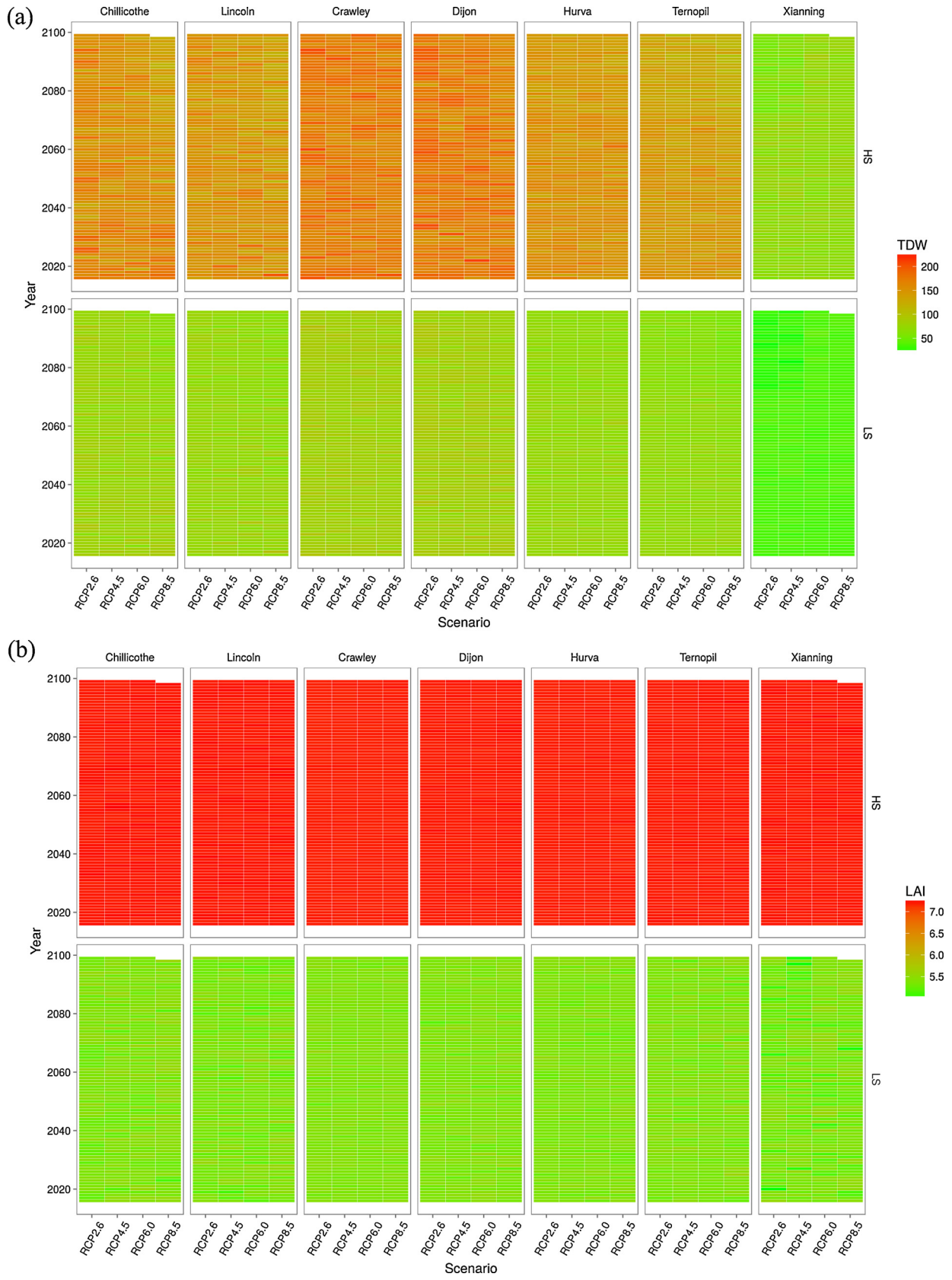

Fig. 2. Heatmaps of plant responses to climate and S conditions under the four climatic scenarios for all the locations. Simulated TDW (a), LAI (b) and QS.mobile.GL (c) at the SED are presented for the locations (top x-axis), under the four RCPs (down x-axis) over years (y-axis) i.e. 5502 situations in total (including simulations with the historical datasets, which are not displayed due to scaling constraints, data in Table 3 and 4).

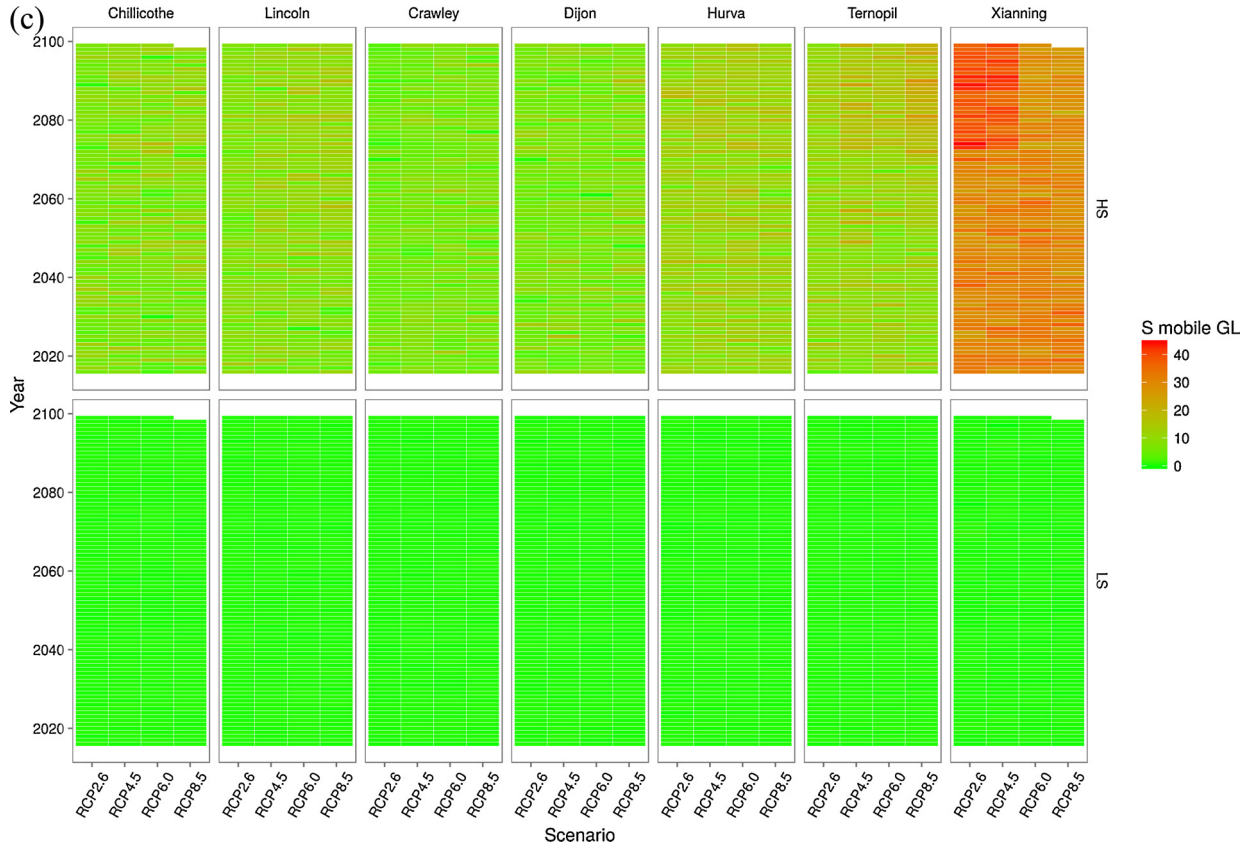

Fig. 2. (*continued*)

S-related variables at the onset of the reproductive phase WOSR. The increase in temperature across years − as expected under the RCP scenarios − brought forward the SED, which is determined by temperature alone (as calibrated in the model). Three location groups can be distinguished in consistence with location groups based on projected temperatures i.e. early SEDs {Chillicothe, Xianning}, intermediate SEDs {Dijon, Lincoln, Ternopil} and late SEDs {Crawley, Hurva}. The location effect on TDW was similar regardless of the S conditions, with {Crawley, Dijon} and {Xianning} having the highest and lowest TDW, respectively. By contrast, the location effect on LDW and LAI was modified according to S conditions with {Lincoln, Xianning, Chillicothe} and {Hurva and Crawley} having the highest and lowest values under HS, respectively, and {Chillicothe, Crawley} and {Xianning} having the highest and lowest values, respectively. Biomass

Table 3
Simulated output values at the SED under HS conditions. Values are the mean of TDW, LAI and QS mobile GL across the years for a given location and a given scenario. Significance was tested among locations for a given scenario and among scenarios (excluding the historical dataset) for a given location. Levels of significance: ns non-significant, * $p < 0.05$, ** $p < 0.01$, *** $p < 0.001$.

Location	Chillicothe	Lincoln	Crawley	Dijon	Hurva	Ternopil	Xianning	
Scenario	TDW (g/plant)							*Location effect*
Historical	162.4	153.5	188.5	180.1	172.9	157.2	98.1	***
RCP2.6	157.2	148.5	171.5	173.2	149.2	140.2	66.8	***
RCP4.5	154.0	146.7	168.3	167.3	146.3	135.5	69.2	***
RCP6.0	151.3	145.8	168.9	169.2	147.0	137.9	71.6	***
RCP8.5	146.9	141.9	165.7	163.9	144.8	132.3	71.9	***
Scenario effect	***	**	***	***	*	***	***	
Scenario	LAI (m^2/m^2)							Location effect
Historical	7.192	7.194	7.174	7.183	7.177	7.182	7.193	***
RCP2.6	7.192	7.196	7.178	7.187	7.183	7.187	7.196	***
RCP4.5	7.194	7.194	7.179	7.188	7.185	7.189	7.192	***
RCP6.0	7.194	7.195	7.179	7.187	7.184	7.189	7.194	***
RCP8.5	7.196	7.196	7.181	7.191	7.184	7.191	7.195	***
Scenario effect	ns	ns	ns	*	ns	ns	ns	
Scenario	QS mobile GL (mg S/plant)							Location effect
Historical	5.37	5.67	3.09	3.58	5.76	4.64	18.38	***
RCP2.6	7.05	7.78	5.29	6.45	10.71	10.31	32.68	***
RCP4.5	8.19	9.20	6.58	6.86	11.86	12.65	32.57	***
RCP6.0	7.84	9.22	6.60	6.47	12.27	11.94	29.95	***
RCP8.5	8.48	9.70	6.60	7.60	11.10	13.67	29.19	***
Scenario effect	*	***	***	*	**	***	***	

Table 4
Simulated output values at the SED under LS conditions. Values are the mean of TDW, LAI and QS mobile GL across the years for a given location and a given scenario. Significance was tested among locations for a given scenario and among scenarios (excluding the historical dataset) for a given location. Levels of significance: ns non-significant, * $p < 0.05$, ** $p < 0.01$, *** $p < 0.001$.

Location	Chillicothe	Lincoln	Crawley	Dijon	Hurva	Ternopil	Xianning	
Scenario	TDW (g/plant)							Location effec
Historical	81.29	77.18	93.68	90.11	85.83	79.47	49.92	***
RCP2.6	78.85	74.94	85.45	85.73	73.54	69.79	34.09	***
RCP4.5	77.45	73.57	83.28	83.20	71.80	67.35	35.24	***
RCP6.0	76.47	73.13	83.59	84.42	72.16	68.46	36.67	***
RCP8.5	74.54	71.19	82.37	81.77	71.53	65.75	36.82	***
Scenario effect	***	**	**	**	*	***	***	
Scenario	LAI (m^2/m^2)							Location effect
Historical	5.379	5.378	5.407	5.402	5.407	5.415	5.425	***
RCP2.6	5.380	5.374	5.413	5.386	5.394	5.399	5.347	***
RCP4.5	5.405	5.372	5.399	5.394	5.381	5.396	5.351	***
RCP6.0	5.401	5.366	5.398	5.409	5.382	5.388	5.374	***
RCP8.5	5.427	5.395	5.412	5.402	5.390	5.399	5.372	**
Scenario effect	*	ns	ns	ns	ns	ns	ns	
Scenario	QS mobile GL (mg S/plant)							Location effect
Historical	0.44	0.47	0.42	0.41	0.45	0.45	0.30	***
RCP2.6	0.42	0.43	0.38	0.37	0.40	0.43	0.37	*
RCP4.5	0.45	0.43	0.39	0.37	0.40	0.41	0.37	***
RCP6.0	0.42	0.45	0.40	0.39	0.38	0.41	0.33	***
RCP8.5	0.45	0.42	0.40	0.39	0.37	0.44	0.34	***
Scenario effect	ns	ns	ns	ns	ns	ns	ns	

allocation to the leaves decreased under S limitation as expected under any mineral constraints, which favours the development of the root system (which is included in the rest of the plant, as calibrated in the model). Therefore, distinct location groups were observed for TDW and LAI according to S conditions. However, another impacting factor inherent to increased temperature is water stress which effect could be even higher than the solely effect of S limitation. Because it is also dependant on the soil properties differing amongst location, location ranking might be impacted under water limitation. With regard to the scenario effect, SED and whole plant biomass were more impacted because the scenario is pessimistic (in a gradual ranking RCP2.6 < RCP4.5 < RCP6.0 < RCP8.5). Expectedly, reduced SED and TDW were observed whatever the S conditions. However, no scenario effect was observed in leaves (except for Dijon under HS and Chillicothe under LS) meaning that overall the biomass allocation processes are not impacted by the projected temperature and incident PAR variation magnitude.

Finally, when comparing the scenarios, lower inter-annual variability on SED was observed because the scenario is more pessimistic as a consequence of a lower magnitude of variation in temperature between years during the simulation period. This implies that model outputs are less subjected to inter-annual variability under more pessimistic scenarios (Fig. 2a–d).

4.2. Impact of warmer temperatures on the shortening of the crop cycle and on plant biomass

In agreement with projected increased temperatures over the coming decades, simulations highlighted an acceleration of the WOSR cycle, with earlier dates for the onset of pod formation (for a cumulative thermal time of 950 °Cd as calibrated in the model). This effect was even more pronounced for locations and scenarios under which the predicted temperatures are high and significantly increased over years (for Chillicothe and Xianning especially under the most pessimistic scenarios i.e. RCP8.5). As a consequence, warmer temperatures from the end of winter until the onset of pod formation lead to shortening of the period of light interception, which would thus impact on global carbohydrate production. In line with this theoretical view, simulations confirmed a decrease in total biomass along with increasing temperatures, especially in Chillicothe and Xianning, which have both early SEDs and low total biomass under the most pessimistic scenarios in particular. Because carbohydrate production at the onset formation is determinant for the development of growing sinks such as pods and seeds, the length of time for radiation interception from the end of winter until the beginning of the reproductive phase is a major controlling factor. Previous *in vivo* studies pointed out similar effects of high temperatures when they occurred from flowering until seed maturity, with lower final performances (e.g. seed yield, seed number and pod number per plant and individual seed dry weight, Brunel-Muguet et al., 2015a). Modifications of seed quality related criteria (such as oil content) highly depend on whether the plants undergo a single stress (increased temperatures, in Brunel-Muguet et al., 2015a) or double stresses (increased temperatures along with higher accumulation of intercepted PAR (Aguirrezábal et al., 2014; Dosio et al., 2000; Izquierdo et al., 2008)). When combined, total oil content increases significantly while the single increase in temperature leads to its reduction. In our study, although Chillicothe and Xianning have similar projected temperature patterns, the daily incident PAR was contrasting, thus leading to different biomasses at the onset of pod formation. Thus different seed oil content could be expected from these simulated results based on earlier plant behaviours.

4.3. Impact on S storage within the plant and environmental issues

S storage is highly determined by S conditions, which represent the effective S taken up by the plant (as parameterized in the model). However, our results highlighted a significant discrepancy under non-limiting S conditions between Xianning and the other locations, with the leaves at Xianning having a three times higher mobile S in the leaves and half the total biomass (regardless of the scenarios). As previously discussed, the projected daily incident PAR is very low and led to reduced total biomass at Xianning. Low incident PAR has a direct effect on photosynthesis and consequently on the production of biomass. As a result, the full amount of S taken up by the plant cannot be assimilated into carbohydrates, which led to S accumulation in the leaves in the mineral form (mobile S in the GL). Simulations in Xianning illustrated how lower incident PAR and warmer temperatures can affect biomass production and in turn S accumulation in the plant. This raises the question of the adjustment of S fertilization when the combination of temperature and radiation are not adequate i.e. high temperature

and low incident PAR. If not adjusted, risks of over-fertilization can occur leading to environmental issues. S excess in the plant is not toxic, in contrast to N over fertilization (with accumulation of ammonia and urea) (Arkoun et al., 2013; Qin et al., 2011), but the detachment of leaves with high residual sulphate during both sequential and monocarpic senescence (which occurs during the vegetative and the reproductive phases, respectively), leads to S losses to the soil, which then risks leaching of S if wetter soil conditions occur.

4.4. Directions for S management and adapted varieties

This simulation study raises questions about S fertilization monitoring and the use of varieties best adapted to the projected higher temperatures that are expected to shift the crop cycle and reduce the length time for radiation interception. First, in light of the contrasting biomass and leaf S storage outputs, S fertilization seems to require adjustments under warm temperatures and low incident radiation, as expected under the four RCP scenarios for the seven tested locations. Beyond economic savings, decreasing the S levels under unfavourable conditions would help to prevent S losses from senescing leaves, and in turn lower the potential leaching of S from the soil. Although S fertilization has gained attention due to observed soil S oligotrophy during recent decades, S fertilization management has adhered to outdates recommendations (i.e. 75 units of SO_3 applied once at the end of winter, Terre Inovia, http://www.terresinovia.fr/colza/cultiver-du-colza/fertilisation/soufre/). Fractioning the S inputs could be tested in order to allow better adjustment to actual biomass production from the end of winter until the reproductive phase. Secondly, varieties with shorter developmental stages, especially from stem elongation (at the end of winter) until pod formation could be of interest because they would be better adapted to a shorter length of time for radiation capture. Thus, varieties with high radiation use efficiency and/or radiation interception efficiency could be targeted. Because spring varieties have a shorter crop cycle and do not have a vernalization requirement, their use under the expected warmer temperatures during spring in the northern hemisphere could be more widely spread, thus delaying sowing to late winter-early spring and harvesting to mid or late summer, which is earlier than winter varieties cultivated in the northern hemisphere. This would also impact on the sowing date of the following crops and hence rotation schemes. In this context, the simulations performed with the model might be used to further adjust farming practices that would be better adapted to the expected climate change. However, careful framing of this study is required because the current version of the model does not take into account expected trends of other major environmental factors that also impact crop yield such as elevated CO_2 concentration, drought or flooding. Interactions might alleviate negative impacts, as demonstrated in previous modelling studies that have indicated higher crop yields in temperate areas where a *ca.* 1–3 °C increase in temperature (i.e. in the first half of the century) would occur alongside CO_2 increases and rainfall pattern modifications (IPCC, 2014; Tubiello et al., 2007). In this context of simultaneous increased CO_2 and temperature, it can be assumed that S storage would be increased as a consequence of higher sink-size (leaf) than under the solely effect of increased temperature (Clausen et al., 2011; Franzaring et al., 2011, 2008).

5. Conclusion

This *in silico* study quantified the impacts of contrasting S supplies along with two crucial environmental factors associated with climate change (i.e. temperature and radiation) on growth and S accumulation at the onset of pod formation in WOSR. Spanning locations across the northern hemisphere and the four RCP scenarios projected during the course of this century, the simulations open avenues for adjustment of S fertilization strategies in terms of amounts, timing and fractioning, according to variety-specific characteristics (ontology and architectural features) and to diverse cropping system designs (e.g. rotation or intercropping) that will be better adapted to ongoing and projected climate change.

Acknowledgements

The authors thank Sébastien Lafont and Olivier Cantat for their help in daily global weather data acquisition and Laurence Cantrill for his help in writing this article. The authors also thank the reviewers for their helpful comments which helped to improve the manuscript. This work was performed in partnership with SAS PIVERT, within the framework of the French Institute for Energy Transition (Institut pour la Transition Energétique (ITE) P.I.V.E.R.T. (www.institut-pivert.com)) selected as an Investment for the Future ("Investissements d'Avenir"). This work was supported by the French Government as part of an Investment for the Future under the reference ANR-001-01.

Appendix A. Supplementary data

Supplementary data associated with this article can be found, in the online version, at https://doi.org/10.1016/j.eja.2018.05.001.

References

Aguirrezábal, L., Martre, P., Pereyra-Irujo, G., Echarte, M.M., Izquierdo, N., 2014. Improving grain quality: ecophysiological and modeling tools to develop management and breeding strategies. Crop Physiology: Applications for Genetic Improvement and Agronomy, second edition. pp. 423–465. http://dx.doi.org/10.1016/B978-0-12-417104-6.00017-0.

Arkoun, M., Jannin, L., Laîné, P., Etienne, P., Masclaux-Daubresse, C., Citerne, S., Garnica, M., Garcia-Mina, J.M., Yvin, J.C., Ourry, A., 2013. A physiological and molecular study of the effects of nickel deficiency and phenylphosphorodiamidate (PPD) application on urea metabolism in oilseed rape (Brassica napus L.). Plant Soil 362, 79–92. http://dx.doi.org/10.1007/s11104-012-1227-2.

Belda, M., Holtanová, E., Halenka, T., Kalvová, J., Hlávka, Z., 2015. Evaluation of CMIP5 present climate simulations using the K??ppen-Trewartha climate classification. Clim. Res. 64, 201–212. http://dx.doi.org/10.3354/cr01316.

Brunel-Muguet, S., D'Hooghe, P., Bataillé, M.-P., Larré, C., Kim, T.-H., Trouverie, J., Avice, J.-C., Etienne, P., Dürr, C., 2015a. Heat stress during seed filling interferes with sulfur restriction on grain composition and seed germination in oilseed rape (Brassica napus L.). Front. Plant Sci. 6, 213. http://dx.doi.org/10.3389/fpls.2015.00213.

Brunel-Muguet, S., Mollier, A., Kauffmann, F., Avice, J.-C., Goudier, D., Sénécal, E., Etienne, P., 2015b. SuMoToRI, an ecophysiological model to predict growth and sulfur allocation and partitioning in oilseed rape (Brassica napus L.) until the onset of pod formation. Front. Plant Sci. 6, 993. http://dx.doi.org/10.3389/fpls.2015.00993.

Challinor, A.J., Müller, C., Asseng, S., Deva, C., Nicklin, K.J., Wallach, D., Vanuytrecht, E., Whitfield, S., Ramirez-Villegas, J., Koehler, A.K., 2017. Improving the use of crop models for risk assessment and climate change adaptation. Agric. Syst. http://dx.doi.org/10.1016/j.agsy.2017.07.010. (1-0).

Chenu, K., Porter, J.R., Martre, P., Basso, B., Chapman, S.C., Ewert, F., Bindi, M., Asseng, S., 2017. Contribution of crop models to adaptation in wheat. Trends Plant Sci. 22 (6), 472–490. http://dx.doi.org/10.1016/j.tplants.2017.02.003.

Clausen, S.K., Frenck, G., Linden, L.G., Mikkelsen, T.N., Lunde, C., Jørgensen, R.B., 2011. Effects of single and multifactor treatments with elevated temperature, CO2 and ozone on oilseed rape and barley. J. Agron. Crop Sci. 197, 442–453. http://dx.doi.org/10.1111/j.1439-037X.2011.00478.x.

D'Hooghe, P., Dubousset, L., Gallardo, K., Kopriva, S., Avice, J.-C., Trouverie, J., 2014. Evidence for proteomic and metabolic adaptations associated to alterations of seed yield and quality in sulphur-limited Brassica napus L. Mol. Cell. Proteomics 13, 1165–1183. http://dx.doi.org/10.1074/mcp.M113.034215.

Dosio, G.A.A., Aguirrezábal, L.A.N., Andrade, F.H., Pereyra, V.R., 2000. Solar radiation intercepted during seed filling and oil production in two sunflower hybrids. Crop Sci. 40, 1637–1644. http://dx.doi.org/10.2135/cropsci2000.4061637x.

Dubousset, L., Etienne, P., Avice, J.C., 2010. Is the remobilization of S and N reserves for seed filling of winter oilseed rape modulated by sulphate restrictions occurring at different growth stages? J. Exp. Bot 61, 4313–4324. http://dx.doi.org/10.1093/jxb/erq233.

Dufresne, J.L., Foujols, M.A., Denvil, S., et al., 2013. Climate change projections using the IPSLCM5 earth system model from CMIP3 to CMIP5. Clim. Dyn. 40 (9–10), 2123–2165. http://dx.doi.org/10.1007/s00382-012-1636-1.

Franzaring, J., Högy, P., Fangmeier, A., 2008. Effects of free-air CO2 enrichment on the growth of summer oilseed rape (Brassica napus cv. Campino). Agric. Ecosyst. Environ. 128, 127–134. http://dx.doi.org/10.1016/J.AGEE.2008.05.011.

Franzaring, J., Weller, S., Schmid, I., Fangmeier, A., 2011. Growth, senescence and water use efficiency of spring oilseed rape (Brassica napus L. cv. Mozart) grown in a factorial combination of nitrogen supply and elevated CO2. Environ. Exp. Bot. 72, 284–296. http://dx.doi.org/10.1016/J.ENVEXPBOT.2011.04.003.

Godfray, H.C.J., Beddington, J.R., Crute, I.R., Haddad, L., Lawrence, D., Muir, J.F., Pretty, J., Robinson, S., Thomas, S.M., Toulmin, C., 2010. Food security: the challenge of feeding 9 billion peopl. Science (80-.) 327, 812–818. http://dx.doi.org/10.1126/science.1185383.

Hawkins, E., Osborne, T.M., Ho, C.K., Challinor, A.J., 2013. Calibration and bias correction of climate projections for crop modelling: an idealised case study over Europe. Agric. For. Meteorol. 170, 19–31. http://dx.doi.org/10.1016/j.agrformet.2012.04.007.

IPCC, 2014. Climate Change 2014: Synthesis Report. Contribution of Working Groups I, II and III to the Fifth Assessment Report of the Intergovernmental Panel on Climate Change, Core Writing Team, R.K. Pachauri and L.A. Meyer. IPCC. 10.1017/CBO9781107415324.004.

Inman, M., 2011. Opening the future. Nat. Clim. Chang. 1, 7–9. http://dx.doi.org/10.1038/nclimate1058.

Izquierdo, N.G., Dosio, G.A.A., Cantarero, M., Luján, J., Aguirrezábal, L.A.N., 2008. Weight per grain, oil concentration, and solar radiation intercepted during grain filling in black hull and striped hull sunflower hybrids. Crop Sci. 48, 688–699. http://dx.doi.org/10.2135/cropsci2007.06.0339.

Lancashire, P.D., Bleiholder, H., Van Den Boom, T., Langelüddeke, P., Stauss, R., Weber, E., Witzenberger, A., 1991. A uniform decimal code for growth stages of crops and weeds. Ann. Appl. Biol. 119, 561–601. http://dx.doi.org/10.1111/j.1744-7348.1991.tb04895.x.

Maiorano, A., Martre, P., Asseng, S., Ewert, F., Müller, C., Rötter, R.P., Ruane, A.C., Semenov, M.A., Wallach, D., Wang, E., Alderman, P.D., Kassie, B.T., Biernath, C., Basso, B., Cammarano, D., Challinor, A.J., Doltra, J., Dumont, B., Rezaei, E.E., Gayler, S., Kersebaum, K.C., Kimball, B.A., Koehler, A.K., Liu, B., O'Leary, G.J., Olesen, J.E., Ottman, M.J., Priesack, E., Reynolds, M., Stratonovitch, P., Streck, T., Thorburn, P.J., Waha, K., Wall, G.W., White, J.W., Zhao, Z., Zhu, Y., 2017. Crop model improvement reduces the uncertainty of the response to temperature of multi-model ensembles. F. Crop. Res. 202, 5–20. http://dx.doi.org/10.1016/j.fcr.2016.05.001.

McGrath, S.P., Zhao, F.J., Blake-Kalff, M.M., 2002. History and outlook for sulphur fertilizers in {Europe}. Fertil. Fertil. 2, 5–27.

Oenema, O., Postma, R., 2003. Managing Sulphur in Agroecosystems, In: Sulphur in Plants. Springer, Netherlands, Dordrecht, pp. 45–70. http://dx.doi.org/10.1007/978-94-017-0289-8_3.

Qin, C., Yi, K., Wu, P., 2011. Ammonium affects cell viability to inhibit root growth in Arabidopsis. J. Zhejiang Univ. Sci. B 12, 477–484. http://dx.doi.org/10.1631/jzus.B1000335.

R Core Team, R: A language and environment for statistical computing [Internet]. Vienna, Austria: R foundation for statistical computing, 2014. Available: http://www.R-project.org/.

Ross, D.J., Newton, P.C.D., Tate, K.R., 2004. Elevated [CO 2] effects on herbage production and soil carbon and nitrogen pools and mineralization in a species-rich, grazed pasture on a seasonally dry sand. Plant Soil 183–196. http://dx.doi.org/10.1023/B:PLSO.0000030188.77365.46.

Ruane, A.C., Teichmann, C., Arnell, N.W., Carter, T.R., Ebi, K.L., Frieler, K., Goodess, C.M., Hewitson, B., Horton, R., Kovats, R.S., Lotze, H.K., Mearns, L.O., Navarra, A., Ojima, D.S., Riahi, K., Rosenzweig, C., Themessl, M., Vincent, K., 2016. The vulnerability, impacts, adaptation and climate services advisory board (VIACS AB v1.0) contribution to CMIP6. Geosci. Model Dev. 9, 3493–3515. http://dx.doi.org/10.5194/gmd-9-3493-2016.

Scherer, H.W., 2001. Sulphur in crop production − invited paper. Eur. J. Agron. http://dx.doi.org/10.1016/S1161-0301(00)00082-4.

Schneider, M.K., Lüscher, A., Richter, M., Aeschlimann, U., Hartwig, U.A., Blum, H., Frossard, E., Nösberger, J., 2004. Ten years of free-air CO2 enrichment altered the mobilization of N from soil in Lolium perenne L. swards. Glob. Chang. Biol. 10, 1377–1388. http://dx.doi.org/10.1111/j.1365-2486.2004.00803.x.

Schnug, E., Evans, E., 1992. Monitoring the sulphur supply of agricultural crops in northern Europe. Phyton 32, 119–122.

Schnug, E., Haneklaus, S., Murphy, D., 1993. Impact of sulphur fertilization on fertilizer nitrogen efficiency. Sulphur Agric. 17, 8–12.

Sheffield, J., Goteti, G., Wood, E.F., 2006. Development of a 50-year high-resolution global dataset of meteorological forcings for land surface modeling. J. Clim. 19, 3088–3111. http://dx.doi.org/10.1175/JCLI3790.1.

Sundström, J.F., Albihn, A., Boqvist, S., Ljungvall, K., Marstorp, H., Martiin, C., Nyberg, K., Vågsholm, I., Yuen, J., Magnusson, U., 2014. Future threats to agricultural food production posed by environmental degradation, climate change, and animal and plant diseases − a risk analysis in three economic and climate settings. Food Secur. 6, 201–215. http://dx.doi.org/10.1007/s12571-014-0331-y.

Tubiello, F.N., Soussana, J.-F., Howden, S.M., 2007. Crop and pasture response to climate change. Proc. Natl. Acad. Sci. 104, 19686–19690. http://dx.doi.org/10.1073/pnas.0701728104.

Von Der Haar, D., Müller, K., Bader-Mittermaier, S., Eisner, P., 2014. Rapeseed proteins −Production methods and possible application ranges. Oilseeds fats Crop. Lipids 21, 1–8. http://dx.doi.org/10.1051/ocl/2013038.

Wang, E., Martre, P., Zhao, Z., Ewert, F., Maiorano, A., Rötter, R.P., et al., 2017. The uncertainty of crop yield projections is reduced by improved temperature response functions. Nat. Plants 3, 17102. http://dx.doi.org/10.1038/nplants.2017.102.

Zhao, F.J., Hawkesford, M.J., McGrath, S.P., 1999. Sulphur assimilation and effects on yield and quality of wheat. J. Cereal Sci. 30, 1–17. http://dx.doi.org/10.1006/jcrs.1998.0241.

van Vuuren, D.P., Edmonds, J., Kainuma, M., Riahi, K., Thomson, A., Hibbard, K., Hurtt, G.C., Kram, T., Krey, V., Lamarque, J.F., Masui, T., Meinshausen, M., Nakicenovic, N., Smith, S.J., Rose, S.K., 2011. The representative concentration pathways: an overview. Clim. Change 109, 5–31. http://dx.doi.org/10.1007/s10584-011-0148-z.